Studies on Dynamic Range of SiPMs with High Pixel Densities

Zhiyu Zhao[3,4,5], *Baohua* Qi[1,2], *Yong* Liu[1,2*], and *Shu* Li[3,4,5]

[1]Institute of High Energy Physics, Chinese Academy of Sciences, 19B Yuquan Road, Beijing, 100049, China
[2]University of Chinese Academy of Sciences, 19A Yuquan Road, Beijing, 100049, China
[3]Tsung-Dao Lee Institute, Shanghai Jiao Tong University, 1 Lisuo Road, Shanghai, 201210, China
[4]Institute of Nuclear and Particle Physics, School of Physics and Astronomy, 800 Dongchuan Road, Shanghai, 200240, China
[5]Key Laboratory for Particle Astrophysics and Cosmology (MOE), Shanghai Key Laboratory for Particle Physics and Cosmology (SKLPPC), Shanghai Jiao Tong University, 800 Dongchuan Road, Shanghai, 200240, China

Abstract. This study examines the dynamic range and saturation behavior of three SiPM models with pixel pitches of 25 μm, 10 μm, and 6 μm, with respective pixel counts of 57,600, 89,984, and 244,719. Using a picosecond laser as the light source and a photomultiplier tube (PMT) operating at different bias voltages as a scaler, we obtained complete response curves of these devices. The results show that SiPMs with 25 μm and 10 μm pixel pitches reached saturation near their nominal pixel counts, while the 6 μm SiPM saturated at about half its nominal count.

1 Introduction

Silicon Photomultipliers (SiPMs) [1, 2] are characterized by their high photon detection efficiency, high gain, insensitivity to magnetic fields, compact structure, and low operating voltages. These devices, composed of an array of avalanche photodiodes (APDs) operating in Geiger mode, enable single-photon detection, initiating a self-sustaining avalanche. SiPMs are widely used in fields such as medical imaging (e.g., PET scans), LIDAR systems, astrophysics, and high-energy physics.

In high-energy collider experiments, calorimeters play a crucial role in accurately measuring particle energy. As the exploration of matter's structure advances, there is an increasing demand for higher-energy colliders and more precise detectors. Scintillation crystal calorimeters, which offer extremely high energy resolution, is widely used in detector systems for collider experiments.

The future Circular Electron-Positron Collider (CEPC) aims to measure the Higgs, W, and Z bosons, top quarks, and explore Beyond Standard Model (BSM) physics [3, 4]. To address challenges in jet reconstruction and achieve optimal electromagnetic energy resolution, a highly granular crystal ECAL with around $3\%/\sqrt{E}$ electromagnetic energy resolution has been proposed for the CEPC [5, 6]. In the conceptual design of this ECAL (Figure 1 (a)), long crystal bars, with BGO as an optional material, are arranged orthogonally between layers to achieve spatial positioning while minimizing the number of readout channels, with SiPMs placed at both ends of the crystal bars as optional photon sensors.

In the CEPC crystal ECAL, the maximum energy deposition in a single crystal bar results from Bhabha scattering of 180 GeV electrons and positrons, corresponding to a 360 GeV center-of-mass energy. To determine the dynamic range of energy deposition in a single crystal bar,

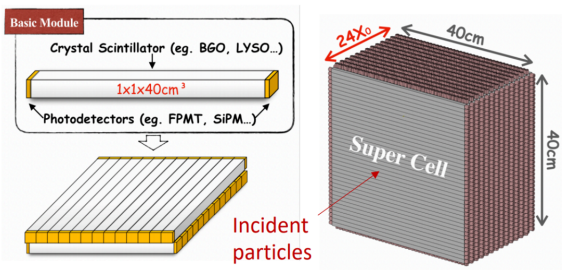

(a)

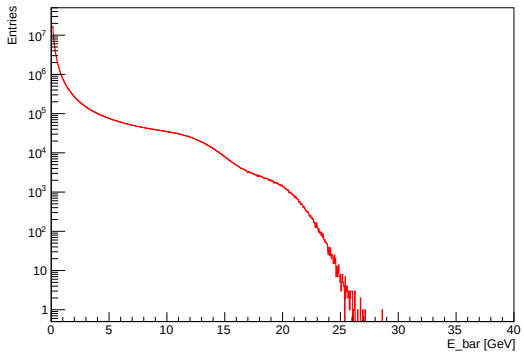

(b)

Figure 1. (a) Structure of the high granularity crystal ECAL. (b) Energy deposition distribution within the ECAL crystal bar for 180 GeV incident electrons.

*e-mail: liuyong@ihep.ac.cn

the ECAL region was scanned with 180 GeV electrons, and the resulting energy distribution for the single crystal is shown in Figure 1 (b). At this energy, a single crystal bar can absorb up to 30 GeV, potentially generating around 350,000 photoelectrons in single channel, placing high demands on SiPM dynamic range.

The dynamic range of SiPMs depends on the number of pixels they contain. Saturation occurs when photon detection exceeds the available pixels, with SiPMs having higher pixel counts exhibiting delayed saturation. Understanding the saturation threshold involves mapping SiPM output across varying light intensities, but requiring calibration with a scaling sensor that maintains linearity—a challenging task. The scaling sensor must operate linearly under strong light input and provide enough gain for accurate calibration. Some experiments use SiPDs with large dynamic ranges but minimal amplification [7], or PMTs with high amplification but small dynamic ranges [8], as scaling sensors. However, the SiPMs tested in these studies typically have pixel counts under 10,000.

We designed an experiment using a PMT to calibrate the incident photon count on the SiPM. The PMT is more likely to saturate than the SiPM under the same light input, but its linear region can be extended by decreasing its bias voltage. By combining linear regions at different biases, we can achieve a linear region for the PMT with the highest possible gain. The dynamic range of three SiPMs with pixel sizes of 25 microns, 10 microns, and 6 microns was tested under laser illumination.

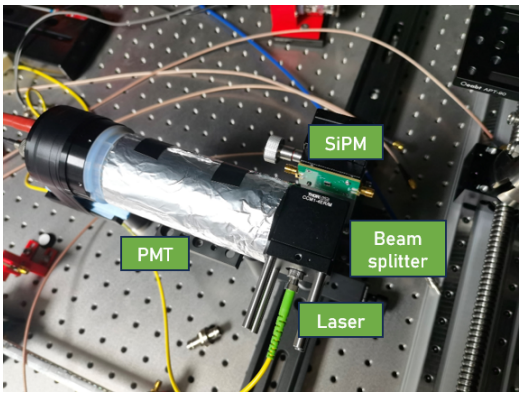

(a)

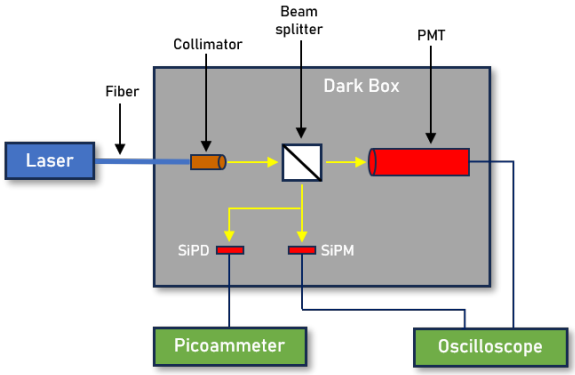

(b)

Figure 2. Diagrams of the experiment setup.

2 Experiment

2.1 Setup

In Figure 2, a picosecond pulsed diode laser (NKT PIL040-FC [9], 405 nm, pulse width within 45 ps) serves as the light source. The emitted light is split into two beams using an optical beam splitter (or alternatively, an integrating sphere), directing one beam to the SiPM under test and the other to the PMT. We evaluated three different SiPM models: two from HAMAMATSU, one with a 25 μm pixel pitch and 57,600 pixels[10], and another with a 10 μm pixel pitch and 89,984 pixels[11], as well as one from NDL with a 6 μm pixel pitch and 244,719 pixels[12]. As listed in Table 1, all featuring a high pixel count.

2.2 Calibration

The gain of a SiPM is the amplification factor that increases the initial charge generated by a single photon. This gain is influenced by factors such as temperature and bias voltage, necessitating individual calibration under controlled conditions. For our experiments, the laboratory temperature was maintained at 25 degrees Celsius by air conditions in the room, and the bias voltage for each SiPM was kept constant as specified in the manual. It should be noted that SiPMs may experience a temperature rise under large signals, but in our experiment, no separate cooling was applied to the SiPMs.

Calibration was conducted with very low incident light intensity, ensuring each pulse emitted only a few photons. The single-photon gain obtained by fitting signals of different photoelectron counts is shown in Table 2.

Saturation in PMTs occurs when the dynodes reach their amplification limits. As light intensity increases, the PMT output plateaus. To reduce susceptibility to saturation, the PMT's gain is lowered by reducing its bias voltage. Several operational modes were developed based on varying bias voltages to optimize gain while preserving a linear response. At low light intensities, the PMT is operated in high bias mode, transitioning to low bias mode as light intensity increases.

In this setup, the incident light is split by a beam splitter, directing one beam to the SiPD and the other to the PMT. The SiPD's output current characterizes the light intensity received by the PMT. Distinct bias voltages were selected for the PMT to accommodate different light intensities, with Figure 3 (a) showing two linear response regions at 600 V and 500 V bias voltages. which are obtained after gain calibration to ensure consistent gain at both voltages.

At 600 V, the PMT's gain was too low to detect single-photon signals. However, in the weak light region, the ratio of charge measurements between the SiPM and PMT remained constant, indicating no saturation in either device. If the number of photoelectrons detected by the PMT matches that of the SiPM in this range, the PMT output

Table 1. Properties of the measured SiPMs.

SiPM Model	Pixel Pitch (μm)	Active Area (mm^2)	Nominal pixel counts	PDE (%) $\lambda = \lambda_p$
HAMAMATSU S13360-6025PE	25	6.0×6.0	57600	25%
HAMAMATSU S14160-3010PS	10	3.0×3.0	89984	18%
NDL EQR06 11-3030D-S	6	3.0×3.0	244719	30%

Table 2. Calibrated QDC-to-p.e. ratios of SiPMs.

S13360-6025PE	S14160-3010PS	EQR06 11-3030D-S
6.42 ns·mV/p.e.	1.69 ns·mV/p.e.	0.9 ns·mV/p.e.

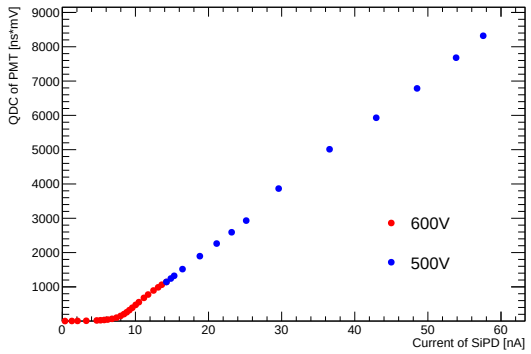

(a)

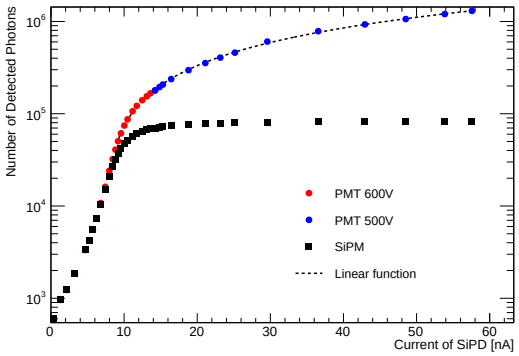

(b)

Figure 3. (a) PMT response at different bias voltages after PMT gain calibration. (b) Response of SiPM and PMT, with a split laser beam illuminating each of them. The PMT output was calibrated by the SiPM in the initial region.

can represent the photon count received by the SiPM. Figure 3 (b) shows the SiPM and PMT responses with the split laser beam. In the low-light region, the data from both devices align. As light intensity increases, the PMT's output remains linear, while the SiPM output begins to saturate. Thus, after calibration, the PMT output can represent the effective photon count the SiPM would detect without saturation effects, equivalent to the product of the SiPM's Photon Detection Efficiency (PDE) and the incident photon count on the SiPM's surface.

2.3 SiPM Response

Figure 4 shows the SiPM response as a function of PMT output. Initially, the SiPM response is nearly linear, but as the light intensity increases, the response deviates from linearity and eventually saturates, with the saturation value approaching SiPM's total pixel counts. This trend is influenced by the time characteristics of the light source. Since the picosecond laser pulse width is much shorter than the SiPM pixel recovery time, each pixel can generate at most one photoelectron per pulse (excluding afterpulses and crosstalk), making the saturation value roughly equal to the SiPM's total pixel counts.

Table 3. Comparison between SiPMs' nominal pixel counts and their maximum photon counts under pico-second laser.

SiPM	Nominal pixel counts	Max. photon counts
S13360-6025PE	57600	51347
S14160-3010PS	89984	82664
EQR06 11-3030D-S	244719	125775

For the HAMAMATSU SiPMs with pixel counts of 57,600 and 89,984, nonlinearity starts at around 7% to 10% of the total pixel counts, with the maximum output under laser illumination slightly below the nominal pixel counts. Ideally, the saturation value should match the pixel count, but due to manufacturing variations, the maximum photon counts detected by the SiPMs under these conditions may fluctuate. Table 3 lists the maximum photon counts detected under laser illumination for each SiPM.

For the NDL SiPM with 244,719 pixels, the measured saturation value is about half of the nominal pixel count, and nonlinearity appears verry early. Similar results were observed in repeated experiments with the same device and other devices of the same type. Further investigation is needed to explain these discrepancies.

3 Conclusions

In this study, we performed a comprehensive evaluation of the intrinsic dynamic range of SiPMs with varying pixel pitches of 6 μm, 10 μm, and 25 μm, each with pixel counts exceeding 50,000. Our experimental results revealed that SiPMs with 25 μm and 10 μm pixel pitches, corresponding to 57,600 and 89,984 pixels respectively, both begin to deviate from linearity in the region where the number of incident photons at approximately 7% to 10% of the total pixel counts, and also exhibited saturation levels that were slightly below their nominal pixel counts. In contrast, the SiPM with a 6 μm pixel pitch and 244,719 pixels showed a

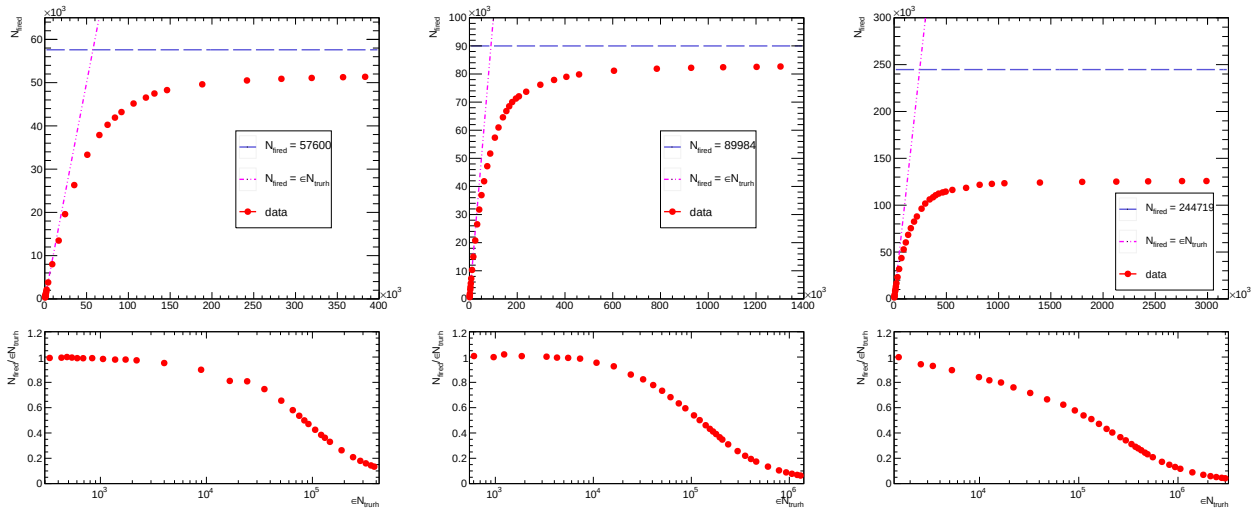

(a) (b) (c)

Figure 4. SiPM response as a function of the effective photon count: (a) HAMAMATSU S13360-6025PE (b) HAMAMATSU S14160-3010PS (c) NDL EQR06 11-3030D-S. In the upper figures, the red points represent the experimental test results, the blue dashed line represents the nominal pixel counts of the SiPM, and the purple dashed line is a slope of one. In the lower figures, the red points represent the ratio of actual photon counts to effective photon counts as measured by SiPM.

saturation point at approximately half of its nominal pixel count, which is not in expectation and need more investigations to unsdertand.

Acknowledgments

This work was supported by National Natural Science Foundation of China (Grant No.: 12150006), National Key R&D Program of China (Grant No.: 2023YFA1606904 and 2023YFA1606900), Shanghai Pilot Program for Basic Research—Shanghai Jiao Tong University (Grant No.: 21TQ1400209), and National Center for High-Level Talent Training in Mathematics, Physics, Chemistry, and Biology.

References

[1] R. Klanner, Characterisation of sipms, Nucl. Instrum. Meth. A **926**, 36 (2019), silicon Photomultipliers: Technology, Characterisation and Applications. https://doi.org/10.1016/j.nima.2018.11.083

[2] F. Simon, Silicon photomultipliers in particle and nuclear physics, Nucl. Instrum. Meth. A **926**, 85 (2019), silicon Photomultipliers: Technology, Characterisation and Applications. https://doi.org/10.1016/j.nima.2018.11.042

[3] T.C.S. Group, Cepc technical design report – accelerator (v2) (2024), 2312.14363, https://arxiv.org/abs/2312.14363

[4] T.C.S. Group, Cepc conceptual design report: Volume 2 - physics detector (2018), 1811.10545, https://arxiv.org/abs/1811.10545

[5] Y. Liu, J. Jiang, Y. Wang, High-granularity crystal calorimetry: conceptual designs and first studies, Journal of Instrumentation **15**, C04056 (2020). 10.1088/1748-0221/15/04/C04056

[6] B. Qi, Y. Liu, R&d of a novel high granularity crystal electromagnetic calorimeter, Instruments **6** (2022). 10.3390/instruments6030040

[7] N. Tsuji, W. Ootani, L. Liu, K. Yoshioka, Y. Morita, M. Gonokami, Study on saturation of SiPM for scintillator calorimeter using UV laser, JINST **15**, C05052 (2020). 10.1088/1748-0221/15/05/C05052

[8] K. Kotera, W. Choi, T. Takeshita, Describing the response of saturated SiPMs (2015), 1510.01102.

[9] N. Photonics, Pil040-fc, https://www.nktphotonics.com/products/pulsed-diode-lasers/pilas/

[10] HAHAMATSU, S13360-6025pe, https://www.hamamatsu.com.cn/cn/zh-cn/product/optical-sensors/mppc/mppc_mppc-array/S13360-6025PE.html

[11] HAHAMATSU, S14160-3010ps, https://www.hamamatsu.com.cn/cn/zh-cn/product/optical-sensors/mppc/mppc_mppc-array/S14160-3010PS.html

[12] N.D. Laboratory, Eqr06 11-3030d-s, http://www.ndl-sipm.net/PDF/Datasheet-EQR06.pdf